Current Sensorless Model Predictive Control of Matrix Converter With Zero Common-Mode Voltage

Ali Sarajian*, Quanxue Guan†, Patrick Wheeler‡, Davood Arab Khaburi§, Ralph Kennel*, Jose Rodriquez¶.
*Institute for High-Power Converter Systems, Technical University of Munich, Germany.
†School of Intelligent Systems Engineering, Sun Yat-Sen University, Guangzhou, China.
‡Department of Electrical and Electronics Engineering, University of Nottingham, U.K.
§Department of Electrical and Electronics Engineering, Iran University of Science and Technology, Iran.
¶Faculty of Engineering, Universidad San Sebastian, Santiago, Chile.
Email: ali.sarajian@tum.de, guanqx3@mail.sysu.edu.cn

***Abstract*—To eliminate the common-mode voltage (CMV) for matrix converters, this paper proposes a current sensorless model predictive control with reduced calculation overhead. In contrast to other traditional CMV-reducing methods which use all permissible switching configurations, this method synthesizes the output voltage and the input current with only six rotating vectors that lead to zero CMV. The proposed technique does not need to predict future load currents and source currents for those six rotating vectors, which provides another advantage in term of computation efficiency. Additionally, all current sensors are removed by using a Luenberger state observer instead in the control loop for cost reduction. The effectiveness of the proposed method is evaluated through simulation in different operation conditions.**

***Index Terms*—Matrix converter, model predictive control, Luenberger observer.**

I. Introduction

Matrix converter (MC) consists of nine bidirectional switch arrays without DC-link energy storage elements, which leads to compact and robust design, sinusoidal input/output currents with controllable input power factor [1]–[4]. Over the years, the main challenges to achieve good performance in MCs have been overcome, making MC topology an attractive alternative to conventional Back-to-Back AC-DC-AC converters [5], [6]. The most fundamental technique for MCs is the modulation strategy. After Alesina and Venturini mathematically proved this topology by direct transfer function modulation [7], [8], several new strategies such as scalar modulation, space vector modulation (SVM), carrier-based modulation, direct torque control and model predictive control (MPC) are reported and reviewed in [9]. Nevertheless, MCs need further development to address issues regarding power quality, operation under abnormal conditions, common-mode voltage (CMV), to name a few [10]. Among them, large magnitude and high-frequency variations of CMVs contribute to early winding failures and bearing degradation in machines [11]. As a result, mitigating CMVs in MCs have garnered considerable attention in recent years [12].

Corresponding author: Quanxue Guan. This work has received funding from the National Natural Science Foundation of China under Grant 51707042, and the support of ANID through projects FB0008, 1210208 and 1221293.

CMV-reducing methods in conventional AC/DC/AC converters may involve the use of isolation transformers, active switching techniques, or zero sequence impedance. However, none of them can provide promising solutions in terms of Total Harmonic Distortion (THD) performance, overall size and cost of the system [13]. Hardware-based solutions to achieve zero CMV are normally costly and with low power density [14]. On the other hand, software-based methods to reduce the CMV typically base on the selection and arrangement of switching patterns in the modulation process. Selecting zero vectors [15] or two active vectors that produce reverse effects [16] have been appropriately demonstrated to mitigate CMVs. Another interesting method is presented in [17] which can achieved reduced CMV by using the switch states that connect each input phase to a different output phase, or the switch state that connects all the output phases to the input phase with minimum absolute voltage. Though reduced significantly by the aforementioned software methods, CMV cannot be eliminated yet. An enhanced SVM method to drive MCs for zero CMV is presented in [18]. However, due to the computation complexity, it is difficult to implement this strategy.

Model Predictive Control (MPC) technique is an emerging most popular control that can adapt to system nonlinearities and multi-objective optimization. Finite Control Set MPC (FCS-MPC) is a type of MPC methods taking into account the discrete nature of power converters and solving the optimization problem among a finite number of switching states [19]. It has been widely applied due to its clear concept and easy implementation. FCS-MPC can not only provide fast dynamic response [20], [21], but also reduce CMV without a modulator, discriminating itself from the SVM-based methods. Except the performance evaluation of load currents and source currents, several FCS-MPC methods added weighted information into the cost functions to constrain CMVs [22], [23].

However, the major problem with FCS-MPC for MCs is on the computation overhead since 27-time predictions of load currents and 27-time predictions of input reactive power or source currents are required. Furthermore, the cost function has to be calculated 27 times to find the optimal switching state. The implementation of FCS-MPC for MCs calls for powerful hardware, which limits their industrial applications [24].

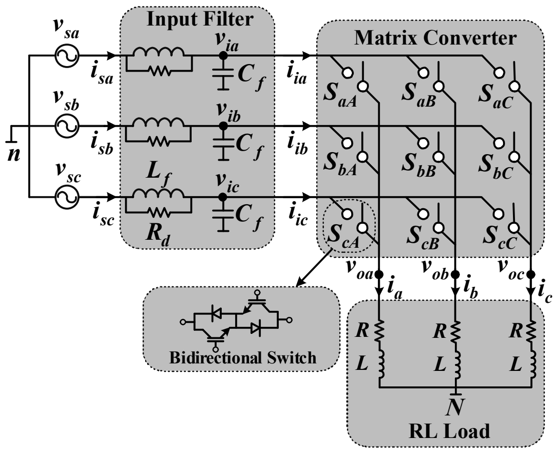

Fig. 1. Topology of a Matrix Converter.

To tackle this problem, *Wang et al.* presented a simplified FCS-MPC to synthesize the output voltage and input current using only the six rotation vectors rather than using all 27 admissible switching configurations [25]. Zero CMV can be achieved. However, the computation overhead is still too high for a general processor, especially a dedicated four-step current-based commutation is necessitated.

Another major concern when the MC topology comes to applications is associated with manufacturing costs. Current sensors directly contribute to that. As a result, the development of sensorless control methods has gained growing attention recently. To avoid using costly current sensors, the sliding mode observer, the Luenberger observer, and the Kalman filter are used instead for state estimation [26], [27]. Kalman filters require a number of numerical computations, including recursive optimization and matrix inversion. The sliding mode observer uses less time because it only requires a sign calculation and a gain multiplication. Luenberger observer only requires a gain multiplication, requiring less computation than the other two observers [28].

This paper presents a further simplification of FCS-MPC to obtain zero CMV for MCs based on [25]. Instead of predicting load currents and source currents for all six rotating vectors, the proposed strategy requires only two prediction calculations for the reference load voltage and the reference input current of MCs. Furthermore, the proposed method differs from the previous MPC by diminishing the current sensor requirements for MCs with a Luenberger observer. The observer is designed to precisely estimate the load current and the source current under a wide range of operating conditions. As a result, the proposed FCS-MPC can substantially reduce the calculation effort, at the same time eliminate the CMV and ensure good input and output current quality.

II. Typical simplified FCS-MPC for CMV Elimination in MCs

The three-phase to three phase MC under exploration is given in Fig. 1. A three phase voltage source feeds the MC through an input filter which is used to reduce the switching frequency harmonics in the input current. For simplicity, the MC drives a three phase resistive-inductive load.

TABLE I
THE SWITCHING CONFIGURATIONS USED IN THE PROPOSED FCS-MPC TO ELIMINATE CMV IN MCS.

	Switching Configuration			Output Voltage	Input Current
State	A	B	C	v_o	i_i
+10	a	b	c	$\lvert v_i \rvert$	$\lvert i_o \rvert$
-10	a	c	b	$\lvert v_i \rvert$	$\lvert i_o \rvert$
+11	c	a	b	$\lvert v_i \rvert$	$\lvert i_o \rvert$
-11	b	a	c	$\lvert v_i \rvert$	$\lvert i_o \rvert$
+12	a	c	b	$\lvert v_i \rvert$	$\lvert i_o \rvert$
-12	c	a	b	$\lvert v_i \rvert$	$\lvert i_o \rvert$

Two switching restrictions have to be taken into account since any two input phases of the MC should not be short-circuited due to the voltage source while any output phase of the MC should not be opened-circuited due to the inductive load. Accordingly, 27 switching states are permissible for the MC. They can be categorized into three groups, namely active vectors with variable magnitude but constant direction (±1 to ±9), zero vectors with zero magnitude ($0a-0c$), and rotating vectors with constant magnitude but variable direction (±10 to ±12). The six rotating vectors, as listed in Table I, produce zero CMV inherently, while active vectors and zero vectors contribute toward CMV. The instantaneous value of the CMV can be found as,

$$v_{cm} = \frac{v_{oA} + v_{oB} + v_{oC}}{3} \tag{1}$$

where v_{oA}, v_{oB} ,and v_{oA} are output phase voltages with respect to neutral point of the source. Using the six rotating vectors is commonly utilized in both SVM- and MPC-based methods, and adopted in this work. In the conventional FCS-MPC to obtain zero CMV in a MC, load current and source current are predicted for six rotating vectors, compared with the reference values to determine the best switching state by minimizing the predefined cost function [25]. To predict load current behavior corresponding to the selected voltage vector among six rotating switching configurations, a discrete-time model of the load is required. The load current equation in a stationary reference frame can be expressed as,

$$L\frac{di_o}{dt} = v_o - R\,i_o \tag{2}$$

where R and L are the load resistance and load inductance, respectively. v_o is the MC output phase voltage and i_o is the load current. Using forward-Euler approximation, (2) can be rewritten as,

$$i_{o|sw}(k+1) = (1-\frac{RT_s}{L})i_o(k) + \frac{T_s}{L}v_{o|sw}(k) \tag{3}$$

where $i_o(k)$ and $i_o(k+1)$ are the load currents at instants k and $k+1$, respectively. For $sw \in \{\pm10, \pm11, \pm12\}$, the load currents in the next time interval are predicted by the corresponding output voltages in (3). The used rotating voltage vector can be computed by the voltage relationship from the input to the output of MCs,

$$v_o = \begin{bmatrix} v_{oa} \\ v_{ob} \\ v_{oc} \end{bmatrix} = \begin{bmatrix} S_{aA} & S_{bA} & S_{cA} \\ S_{aB} & S_{bB} & S_{cB} \\ S_{aC} & S_{bC} & S_{cC} \end{bmatrix} \cdot \begin{bmatrix} v_{ia} \\ v_{ib} \\ v_{ic} \end{bmatrix} = S \cdot v_i \quad (4)$$

Similarly, the source currents can be predicted using the discrete-time state-space model of the *RLC* input filter, given as follows,

$$\begin{bmatrix} v_i(k+1) \\ i_s(k+1) \end{bmatrix} = A_d \begin{bmatrix} v_i(k) \\ i_s(k) \end{bmatrix} + B_d \begin{bmatrix} v_s(k) \\ i_i(k) \end{bmatrix}, \quad (5)$$

where

$$A_d = e^{AT_s},\ B_d = \int_0^{T_s} e^{A(T_s-\tau)} B d\tau, \quad (6)$$

$$A = \begin{bmatrix} 0 & \frac{1}{C_f} \\ -\frac{1}{L_f} & -\frac{R_f}{L_f} \end{bmatrix}, B = \begin{bmatrix} 0 & -\frac{1}{C_f} \\ \frac{1}{L_f} & 0 \end{bmatrix}, \quad (7)$$

C_f and L_f are the input filter capacitance and inductance, respectively. R_f is the leakage resistance of L_f. Solving the second line of (5) obtains

$$\begin{aligned} i_{s|sw}(k+1) &= A_d(2,1)v_i(k) + A_d(2,2)i_s(k) \\ &+ B_d(2,1)v_s(k) + B_d(2,2)i_{i|sw}(k) \end{aligned} \quad (8)$$

The source current at instant $k+1$ is a function of the MC input current vector i_i that can be determined from the current relationship of the MC with the help of the rotating switching configurations and the output currents as below,

$$i_i = \begin{bmatrix} i_{ia} \\ i_{ib} \\ i_{ic} \end{bmatrix} = \begin{bmatrix} S_{aA} & S_{aB} & S_{aC} \\ S_{bA} & S_{bB} & S_{bC} \\ S_{cA} & S_{cB} & S_{cC} \end{bmatrix} \cdot \begin{bmatrix} i_a \\ i_b \\ i_c \end{bmatrix} = S^T \cdot i_0 \quad (9)$$

It is assumed that one rotating switching state is applied for one control cycle starting from instant k. The load current and source current at instant $k+1$ are predicted by (3) and (8) and then compared with their respective references to select the optimal switching state. To do this, a classical cost function is formulated as follows:

$$CF_{sw} = |i_o^* - i_o(k+1)| + k_Q\,|i_s^* - i_s(k+1)| \quad (10)$$

where i_s^* and i_o^* are the source current reference value and the load current reference value, respectively. k_Q is a weighting factor that can be set to achieve good tracking performance. The simplified FCS-MPC is realized by evaluating (10) with 6 rotating switching states of the MC and then selecting the state with minimum cost function. As a result, the simplified FCS-MPC for the MC requires 6 times of load current predictions, 6 times of source current predictions, and 6 times of cost function evaluation. Even though the computation overhead is reduced significantly by using less switching configurations, it is still too high for a general digital processor.

III. Proposed FCS-MPC with Zero CMV for MCs

A. Prediction simplification

The proposed method intends to simplify the FCS-MPC for further calculation reduction. Instead of requiring 6 times of load current predictions and 6 times of source current predictions to evaluate the cost functions for instant $k+1$, it uses the desired output voltage vector v_o^* and the input current vector i_i^* for prediction, deriving from (3), (8) and expressing as follows:

$$v_o^*(k) = \frac{L}{T_s}[i_o^*(k+1) - i_o(k)] + Ri_o(k) \quad (11)$$

$$i_i^*(k) = \frac{i_s^*(k+1) - A_d(2,1)v_i(k) - A_d(2,2)i_s(k) - B_d(2,1)v_s(k)}{B_d(2,2)} \quad (12)$$

In accordance with (11), if the voltage vector exerted by the converter onto the load at instant k equals $v_o^*(k)$, then the load current at instant $k+1$ will track its reference current. This work uses only 6 voltage vectors to obtain Zero CMV, which may not match the target voltage vector exactly. Nonetheless, the most appropriate method for reducing the error between the load current and its reference at the end of the next sampling time is to apply the voltage vector that is closest to the desired voltage vector. Similarly, the source current can be controlled using (12). The source current at instant $k+1$ will be the same as the reference source current if the input current vector of the MC at instant k is the same as $i_i^*(k)$. To calculate (11), i_s, v_s and v_i need to be measured by sensors.

Prior to calculating Eq. (12), it is imperative to generate a source current reference. If the converter power losses are neglected, the active input power and output power of MCs are assumed to be equal, $P_{in} = P_{out}$. Thus, by considering sinusoidal nature of reference signal and ensuring unity input power factor, the source current reference of any phase can be calculated from output power, given with phase "a" as below,

$$i_{sa}^* = \left(R \times (i_{oa}^{2\,*} + i_{ob}^{2\,*} + i_{oc}^{2\,*})\right) \times \left(\frac{v_{sa}}{v_{sa}^2 + v_{sb}^2 + v_{sc}^2}\right) \quad (13)$$

The load parameters, reference output currents, and the MC source voltages are required as inputs for this method of determining the MC reference source current.

A cost function is now required to determine the optimal switching state including a combination of the input currents tracking error and the output voltages tracking error simultaneously, which can be revised as follows,

$$CF_{sw} = |v_o^*(k) - v_{o|sw}| + k_Q\,|i_i^*(k) - i_{i|sw}| \quad (14)$$

The one among the 6 rotating switching states that minimizes the cost function (14) is then applied to the MC. Therefore, there is no need to calculate six load current predictions and six source current predictions because one prediction is needed to calculate the output voltage vector, and another prediction is required to calculate the input current vector.

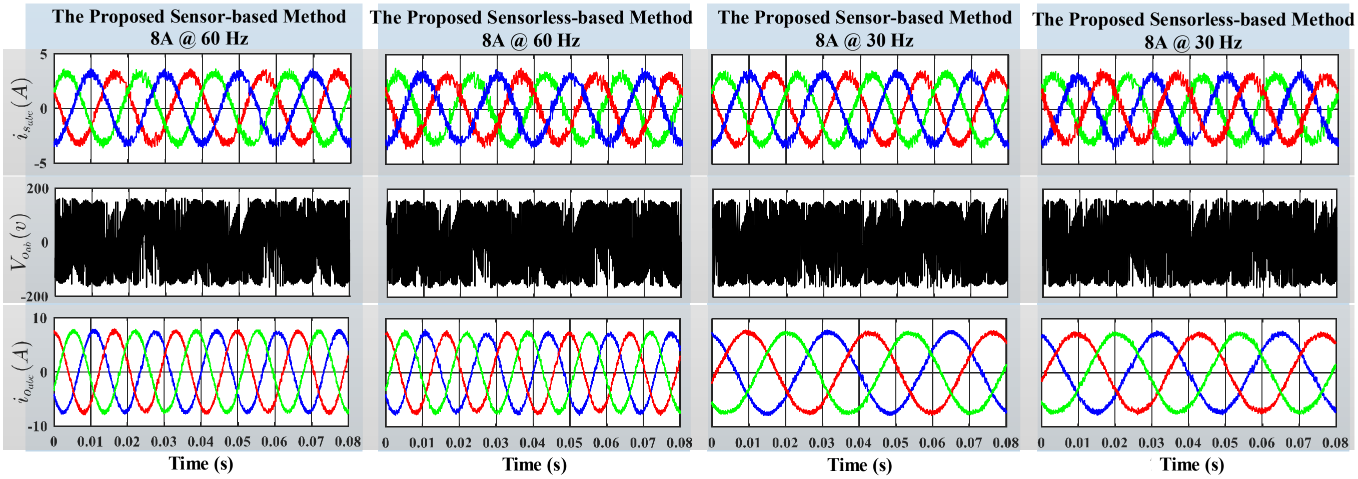

Fig. 2. Steady state performance of the typical sensor-based and the proposed sensorless-based MPCs when ($i_o^* = 8A$ at 60 Hz) and ($i_o^* = 8A$ at 30 Hz).

TABLE II
SYSTEM PARAMETERS

Parameter	Explanation	Value
$L_f(mH)$	Input filter inductance	0.6
$C_f(\mu F)$	Input filter capacitance	66
$R_d(\Omega)$	Damping resistor	9
$L(mH)$	Load Inductance	6.6
$R(\Omega)$	Load resistance	4
$T_s(\mu s)$	Sample time	35
$v_s(v)$	Supply voltage (RMS)	64.2V, 50Hz
k_Q	Weighting factor	50

B. Source Current and load current Estimations

Control algorithms require the voltage and current information from the source and load sides of MCs. To avoid high cost measurement, this work applies a Luenberger observer to estimate the source currents and load currents. These currents are then used in (11) and (12) to calculate the input current reference and output voltage reference, respectively. Implementation of the observer entails the mathematical model of the input filter and RL load of the MC, given as follows,

$$\begin{cases} \frac{di_s}{dt} = \frac{1}{L_f}(v_s(k) - v_i(k) - R_f i_s(k)) \\ \frac{dv_i}{dt} = \frac{1}{C_f}(i_s(k) - i_i(k)) \\ \frac{di_o}{dt} = \frac{1}{L}(v_o(k) - Ri_o(k)) \end{cases} \tag{15}$$

Here, $v_o(k)$ and $i_i(k)$ have been determined by the MC system model $v_o(k) = S \times v_i(k)$ and $i_i(k) = S^T \times i_o(k)$, referring to (4) and (9) respectively. The source currents and load currents are estimated by introducing the following equation,

$$\frac{d}{dt}\begin{bmatrix} \hat{i}_s \\ \hat{v}_i \\ \hat{i}_o \end{bmatrix} = \begin{bmatrix} \frac{1}{L_f}(v_s(k) - v_i(k) - R_f i_s(k)) \\ \frac{1}{C_f}(i_s(k) - i_i(k)) \\ \frac{1}{L}(v_o(k) - Ri_o(k)) \end{bmatrix} + \begin{bmatrix} L_1 \\ L_2 \\ L_3 \end{bmatrix}(v_i - \hat{v}_i) \tag{16}$$

where $\hat{i}_s$, $\hat{v}_i$ and $\hat{i}_o$ represent the estimated source current, input voltage and load current for the MC, respectively. And L_1 , L_2 and L_3 are constant coefficients for the Luenberger estimator. A linearized version of this system around an operating point can be constructed by placing the poles on the left of the imaginary axis, which determines the overall range of the parameters. Adjusting $L_1 = 0.0005$, $L_2 = 1$ and $L_3 = 0.0005$ will result in high accuracy in the simulation.

IV. SIMULATION RESULTS

The feasibility and effectiveness of the proposed method has been tested through simulation using MATLAB/Simulink. For fair comparison, the similar specifications as in [25] are used. The steady state performance of source currents, load voltages, and load currents are depicted in Fig. 2 when the proposed sensorless FCS-MPC method and the typical sensor-based FCS-MPC method as presented in [25] are applied for a load current reference of $8A$ at $60Hz$ and $8A$ at $30Hz$. It is apparent that the proposed methods provide satisfactory performance including sinusoidal load and source current and a nearly unity input power factor. To prove this, the harmonic spectrum of source currents and load currents are represented in Fig. 3. The obtained THD values of the proposed FCS-MPC can be compared to those of the typical simplified FCS-MPC. The THD of i_{sa} and i_{oa} obtained by *Wang et al.* [25] are 12.81% and 5.12% for the case of $8A$ at $30Hz$, and 12.41% and 3.67% for the case of $8A$ at $60Hz$, respectively, while the proposed method has better THD performance, specially for the case of source currents which show a tangible reduction. CMV waveforms under the condition of applying a load current reference $8A$ at $60Hz$ are shown in Fig. 4 for both the typical sensor-based (Fig. 4(a)) and the proposed sensorless-based (Fig. 4(b)) methods.

Further, the dynamics transition of the MC system is tested. Fig. 5 shows the system response when both amplitude and frequency are changed simultaneously. As shown in Fig. 5(a) and (b), the frequency of the load current is varied from $25Hz$

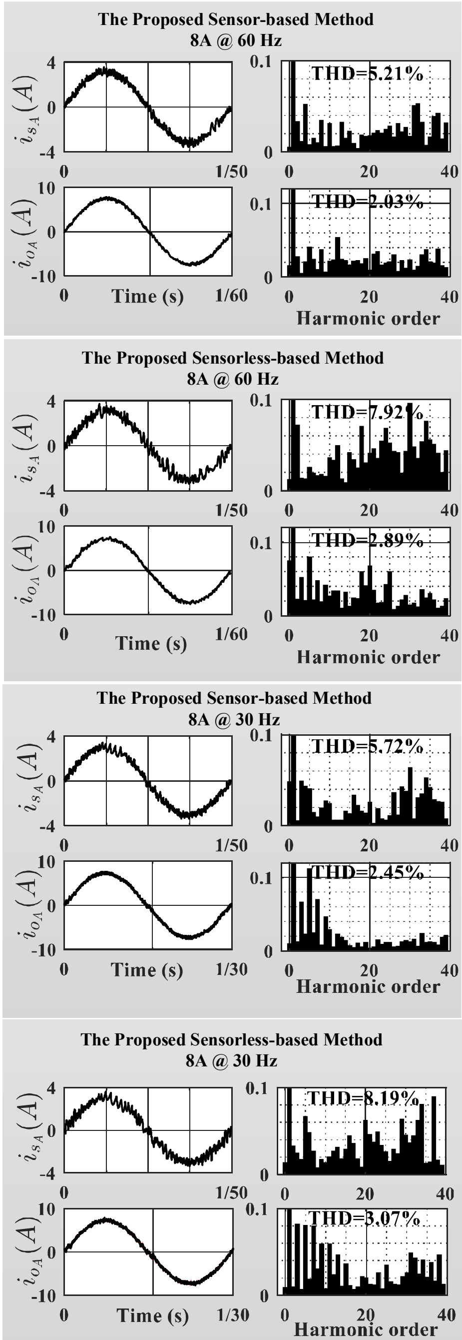

Fig. 3. Harmonic spectrum of source current i_{sa} and load current i_{oa} when the typical sensor-based and the proposed sensorless-based MPCs are used.

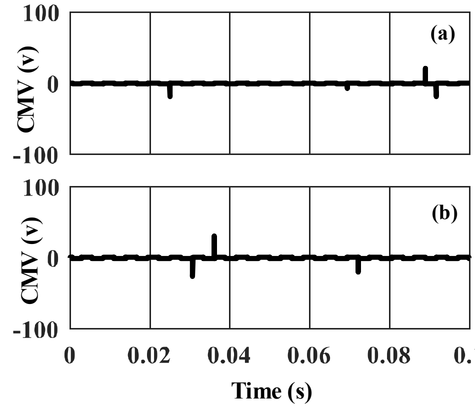

Fig. 4. CMV elimination by using (a) the typical sensor-based MPC, (b) the proposed sensorless-based MPC.

to $50Hz$, and the amplitude from $6A$ to $8A$. Controlled by the typical sensor-based MPC and the proposed sensorless-based MPC, satisfying results are observed. Fig. 5 also represents the effect of varying load current reference on the source side of the system while maintaining near-unity input power factor. The proposed method in this paper shows considerable improvement over the techniques proposed in [25] and [29] in terms of the waveform quality or the THD. It is worth noting that the proposed FCS-MPC scheme does not require switching tables or look-up tables, as compared to previously documented methods.

V. Conclusions

This paper proposes a current sensorless model predictive control method that yields zero CMV by using six rotating vectors as the candidate switching states. Reducing calculation effort is another goal of this method which is successfully obtained by only two predictions of the output voltage reference and input current reference of MC. Additionally, all current sensors have been successfully replaced by a Luenberger state observer to reduce costs without degrading the overall performance of the MC system. Simulation results show that the proposed algorithms by taking full advantage of the MC model (V/I relationships) in the MPC is capable of working effectively with a variety of supply voltage frequencies and output frequencies, improves load/source current quality, and maintains the input power factor at unity.

References

[1] P. Wheeler, J. Rodriguez, J. Clare, L. Empringham, and A. Weinstein, “Matrix converters: a technology review,” *IEEE Trans. Industrial Electronics*, vol. 49, no. 2, pp. 276–288, 2002.

[2] L. Empringham, J. Kolar, J. Rodriguez, W. Patrick, and J. Clare, “Technological issues and industrial application of matrix converters: A review,” *IEEE Trans. Industrial Electronics*, vol. 60, no. 10, pp. 4260–4271, 2013.

[3] H.-N. Nguyen and H.-H. Lee, “An effective svm method for matrix converters with a superior output performance,” *IEEE Trans. Industrial Electronics*, vol. 65, no. 9, pp. 6948–6958, 2017.

[4] O. Simon, J. Mahlein, M. Muenzer, and M. Bruckmarm, “Modern solutions for industrial matrix-converter applications,” *IEEE Trans. Industrial Electronics*, vol. 49, no. 2, pp. 401–406, 2002.

[5] Q. Guan, P. Yang, Q. Guan, X. Wang, and Q. Wu, “A singular value decomposition-based space vector modulation to reduce the output common-mode voltage of direct matrix converters,” *Journal of Power Electronics*, vol. 16, no. 3, pp. 936–945, 2016.

[6] Q. Guan, P. Wheeler, O. Simon, Q. Guan, and J. Clare, “Geometrical visualisation of indirect space vector modulation for matrix converters operating with abnormal supplies,” *IET Power Electronics*, vol. 12, no. 15, pp. 4023–4033, Dec. 2019.

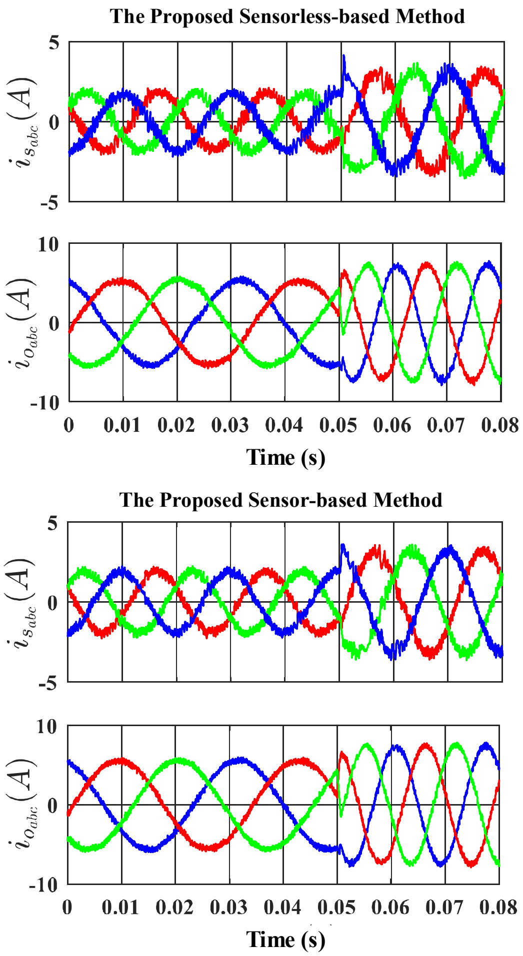

Fig. 5. Dynamic performance of proposed method during change in the frequency and amplitude of load current reference (a) by using the observer (b) by using current sensor

[7] A. Alesina and M. Venturini, "Solid-state power conversion: A fourier analysis approach to generalized transformer synthesis," *IEEE Trans. Circuits and Systems*, vol. 28, no. 4, pp. 319–330, 1981.

[8] Alesina and Venturini, "Analysis and design of optimum-amplitude nine-switch direct AC-AC converters," *IEEE Trans. Power Electronics*, vol. 4, no. 1, pp. 101–112, 1989.

[9] J. Rodriguez, M. Rivera, J. Kolar, and P. Wheeler, "A review of control and modulation methods for matrix converters," *IEEE Trans. Industrial Electronics*, vol. 59, no. 1, pp. 58–70, 2012.

[10] M. Aten, G. Towers, C. Whitley, P. Wheeler, J. Clare, and K. Bradley, "Reliability comparison of matrix and other converter topologies," *IEEE Trans. Aerospace and Electronic systems*, vol. 42, no. 3, pp. 867–875, 2006.

[11] J. M. Erdman, R. J. Kerkman, D. W. Schlegel, and G. L. Skibinski, "Effect of pwm inverters on ac motor bearing currents and shaft voltages," *IEEE Trans. on Industry Applications*, vol. 32, no. 2, pp. 250–259, 1996.

[12] R. Vargas, J. Rodriguez, C. A. Rojas, and M. Rivera, "Predictive control of an induction machine fed by a matrix converter with increased efficiency and reduced common-mode voltage," *IEEE Trans. energy conversion*, vol. 29, no. 2, pp. 473–485, 2014.

[13] S. Wei, N. Zargari, B. Wu, and S. Rizzo, "Comparison and mitigation of common mode voltage in power converter topologies," in *39th IAS Annual Meeting, IEEE Industry Applications Conference, 2004.*, vol. 3. IEEE, 2004, pp. 1852–1857.

[14] S. Nath and N. Mohan, "A matrix converter fed sinusoidal input output three winding high frequency transformer with zero common mode voltage," in *2011 International Conf. Power Engineering, Energy and Electrical Drives*. IEEE, 2011, pp. 1–6.

[15] H.-H. Lee and H. M. Nguyen, "An effective direct-svm method for matrix converters operating with low-voltage transfer ratio," *IEEE Trans. power electronics*, vol. 28, no. 2, pp. 920–929, 2012.

[16] H. J. Cha and P. N. Enjeti, "An approach to reduce common-mode voltage in matrix converter," *IEEE Trans. industry applications*, vol. 39, no. 4, pp. 1151–1159, 2003.

[17] Q. Guan, P. Wheeler, Q. Guan, and P. Yang, "Common-mode Voltage Reduction for Matrix Converters Using All Valid Switch States," *IEEE Trans. Power Electronics*, vol. 31, no. 12, pp. 8247–8259, 2016.

[18] H.-N. Nguyen and H.-H. Lee, "An enhanced svm method to drive matrix converters for zero common-mode voltage," *IEEE Trans. Power Electronics*, vol. 30, no. 4, pp. 1788–1792, 2014.

[19] M. Rivera, A. Wilson, C. A. Rojas, J. Rodriguez, J. R. Espinoza, P. W. Wheeler, and L. Empringham, "A comparative assessment of model predictive current control and space vector modulation in a direct matrix converter," *IEEE Trans. Industrial Electronics*, vol. 60, no. 2, pp. 578–588, 2013.

[20] M. Siami, D. A. Khaburi, and J. Rodriguez, "Simplified finite control set-model predictive control for matrix converter-fed pmsm drives," *IEEE Trans. Power Electronics*, vol. 33, no. 3, pp. 2438–2446, 2017.

[21] A. Sarajian, C. F. Garcia, Q. Guan, P. Wheeler, D. A. Khaburi, R. Kennel, J. Rodriguez, and M. Abdelrahem, "Overmodulation methods for modulated model predictive control and space vector modulation," *IEEE Trans. Power Electronics*, vol. 36, no. 4, pp. 4549–4559, 2020.

[22] R. Vargas, U. Ammann, J. Rodríguez, and J. Pontt, "Predictive strategy to control common-mode voltage in loads fed by matrix converters," *IEEE Trans. industrial electronics*, vol. 55, no. 12, pp. 4372–4380, 2008.

[23] M. Rivera, J. Rodriguez, J. Espinoza, and B. Wu, "Reduction of common-mode voltage in an indirect matrix converter with imposed sinusoidal input/output waveforms," in *38th Annual Conf. IEEE Industrial Electronics Society in IECON 2012*. IEEE, 2012, pp. 6105–6110.

[24] A. Sarajian, Q. Guan, P. Wheeler, D. A. Khaburi, R. Kennel, and J. Rodriquez, "Over-modulation method of modulated model predictive control for matrix converters," in *IECON 2020 The 46th Annual Conference of the IEEE Industrial Electronics Society*, 2020, pp. 4624–4629.

[25] L. Wang, H. Dan, Y. Zhao, Q. Zhu, T. Peng, Y. Sun, and P. Wheeler, "A finite control set model predictive control method for matrix converter with zero common-mode voltage," *IEEE Journal of Emerging and Selected Topics in Power Electronics*, vol. 6, no. 1, pp. 327–338, 2018.

[26] A. Sarajian, D. A. Khaburi, and M. Rivera, "Using extended kalman filter and adaptive filter for sensorles predictive torque control of pm-assissted synchronous reluctance motor," in *7th Power Electronics and Drive Systems Technologies Conference (PEDSTC)*, 2016, pp. 64–69.

[27] M. Mousavi, S. A. Davari, V. Nekoukar, C. Garcia, L. He, F. Wang, and J. Rodriguez, "Predictive torque control of induction motor based on a robust integral sliding mode observer," *IEEE Trans. Industrial Electronics*, pp. 1–1, 2022.

[28] P. Haghgooei, A. Corne, E. Jamshidpour, N. Takorabet, D. A. Khaburi, and B. Nahid-Mobarakeh, "Current sensorless control for a wound rotor synchronous machine based on flux linkage model," *IEEE Journal of Emerging and Selected Topics in Power Electronics*, pp. 1–1, 2021.

[29] M. Siami, D. A. Khaburi, and J. Rodriguez, "Simplified finite control set-model predictive control for matrix converter-fed pmsm drives," *IEEE Trans. Power Electronics*, vol. 33, no. 3, pp. 2438–2446, 2017.